

Probing Triple- W Production and Anomalous $WWWW$ Coupling at the CERN LHC and future $\mathcal{O}(100)$ TeV proton-proton collider

Yiwen Wen^a, Huilin Qu^a, Daneng Yang^a, Qi-shu Yan^b, Qiang Li^a, Yajun Mao^a,

^a*Department of Physics and State Key Laboratory of Nuclear Physics and Technology, Peking University, Beijing, 100871, China*

^b*College of Physics Sciences, University of Chinese Academy of Sciences, Beijing 100049, China and Center for High Energy Physics, Peking University, Beijing 100871, China*

E-mail: wenyw@pku.edu.cn, quhl@pku.edu.cn

ABSTRACT: Triple gauge boson production at the LHC can be used to test the robustness of the Standard Model and provide useful information for VBF di-boson scattering measurement. Especially, any derivations from SM prediction will indicate possible new physics. In this paper we present a detailed Monte Carlo study on measuring $W^\pm W^\pm W^\mp$ production in pure leptonic and semileptonic decays, and probing anomalous quartic gauge $WWWW$ couplings at the CERN LHC and future hadron collider, with parton shower and detector simulation effects taken into account. Apart from cut-based method, multivariate boosted decision tree method has been exploited for possible improvement. For the leptonic decay channel, our results show that at the $\sqrt{s} = 8(14)[100]$ TeV pp collider with integrated luminosity of $20(100)[3000]$ fb⁻¹, one can reach a significance of $0.4(1.2)[10]\sigma$ to observe the SM $W^\pm W^\pm W^\mp$ production. For the semileptonic decay channel, one can have $0.5(2)[14]\sigma$ to observe the SM $W^\pm W^\pm W^\mp$ production. We also give constraints on relevant Dim-8 anomalous $WWWW$ coupling parameters.

KEYWORDS: Triple Gauge Boson Production, Anomalous Quartic Gauge Boson Couplings, MC Simulation, LHC

Contents

1	Introduction	1
2	Effective Interactions for aQGCs	3
3	Standard model $W^\pm W^\pm W^\mp$ production in pure leptonic decay channel	4
3.1	Cut-based method	5
3.2	Multivariate analysis BDT method	6
3.3	Numerical Results	7
4	Standard model $W^\pm W^\pm W^\mp$ production in semileptonic decay channel	8
4.1	Cut-based method	9
4.2	Multivariate analysis BDT method	9
4.3	Numerical results	10
5	Anomalous $WWWW$ Couplings	10
5.1	aQGC in pure leptonic decay channel	10
5.2	aQGC in semileptonic decay channel	12
6	WWW production and aQGC at 100 TeV future pp collider	15
6.1	Pure leptonic decay channel	15
6.2	Semileptonic decay channel	15
6.3	Anomalous quartic couplings	16
7	Unitarity safety discussion	17
8	Conclusion	17

1 Introduction

Since the beginning of the LHC era, no significant deviation from the Standard Model (SM) of particle physics has been observed. Instead, the SM has achieved great success, especially after the recent discovery of a 125-126 GeV Higgs boson in both CMS and ATLAS experiments at the LHC [1–4]. Nevertheless, we still look forward to Beyond Standard Model physics to explain some mysterious facts, such as the existence of dark matter and the electroweak-Plank scales hierarchy problem. Hence, further test on SM and searching for new physics beyond the SM become urgent quests for both theorists and experimentalists. On the other hand, the upgrade of LHC to higher collision energy and luminosity, and the promising plan for future $\mathcal{O}(100)$ TeV proton-proton collider, make it possible to measure various ‘rare’ SM processes, including, e.g. multi-boson productions.

To study anomalous bosonic couplings is one possible way to explore new physics. In the framework of SM, the gauge boson self-interaction is fully determined by the $SU(2)_L \otimes U(1)_Y$ gauge symmetry. Any presences of anomalous couplings may result in observable deviation from SM. To study vector boson interactions, therefore, can either further confirm the SM and the spontaneously symmetry breaking mechanism, or shed a light on new physics.

Extra contributions other than the SM predictions can be induced by possible new physics, which can be expressed in a model independent way by introducing high-dimensional operators which lead to anomalous triple or quartic gauge couplings (aTGCs or aQGCs). The explorations of aTGCs have already been done at the LEP [5, 6], Tevatron [7, 8], and later at the LHC [9, 10] through the dibosons production. Compared with TGCs measurement, triple gauge boson production [11–14], though suffered from lower cross sections and complicated final state topology, is essential for testing QGCs. As discussed in Ref. [15, 16], it is possible that the QGCs deviate from SM prediction while the TGCs do not. For instance, the exchange of extra heavy boson between vector boson can generate tree-level contributions to four gauge boson couplings while the effect on the triple gauge vertex appears only at 1-loop and is accordingly suppressed [15, 16].

As to aQGCs, previous Monte-Carlo (MC) and experimental studies have been carried out at $e\gamma$ and $\gamma\gamma$ colliders [17, 18], linear colliders [15, 19–24], and hadron colliders [16, 25–32]. Many experiments gave direct constraints including LEP, by studying the $WW\gamma$ [21, 23], $Z\gamma\gamma$ [22] and $\gamma\gamma\nu\bar{\nu}(q\bar{q})$ [24] channels, e.g., constraints on $WW\gamma\gamma$ aQGC parameters are given. Recently, CMS presents new results on $WW\gamma\gamma$ and $WWZ\gamma$ aQGCs by studying the semi-leptonic $WV\gamma$ production [30] and $\gamma\gamma \rightarrow WW$ channel [31]. ATLAS has studied $WWWW$ aQGC via the same sign WW channel [32].

In the next few years, the LHC at CERN will be upgraded with higher center-of-mass energy and luminosity and it is expected that it will set more strict constraints on aQGCs. The MC studies on $W^+W^-\gamma$ [33] production and $W^\pm Z\gamma$ production [34] have confirmed the potential of LHC on probing $WW\gamma\gamma$ and $WWZ\gamma$ aQGCs. As to $WWWW$ vertices, Eboli *et al.* [35] studied on the vector boson fusion (VBF) WW channel and set the aQGC parameter $f_{S0,S1}$ constraints at the order of 10^{-11}GeV^{-4} at 99% CL with integrated luminosity of 100 fb^{-1} . Preliminary result from Snowmass [36] via the $W^\pm W^\pm W^\mp$ production pure leptonic channel set the aQGC parameter f_{T0}/Λ^4 at the order of 10^{-12} GeV^{-4} at 5σ with 300 fb^{-1} 14 TeV LHC.

This paper will present detailed study on triple gauge boson production via exploring the potential of measuring $W^\pm W^\pm W^\mp$ final states with full leptonic decay and semileptonic decay at the $\sqrt{s} = 8$ and 14 TeV CERN LHC and future proton-proton collider, and probing the $WWWW$ anomalous coupling. Our work extends Eboli *et al.* and Snowmass’ study as an independent test on triple electroweak gauge boson physics. We begin by introducing the aQGC related effective theory and specifying the effective Lagrangian in Sec. 2, and then present our MC simulation on SM WWW production with pure leptonic decay channel in Sec. 3 and semileptonic channel in Sec. 4. In Sec. 5, we demonstrate the result on the $WWWW$ aQGC study. The WWW production and aQGC at 100 TeV hadron collider analysis will be given in Sec. 6. Unitarity safety on the aQGC limits is discussed in Sec. 7.

Finally, we draw our conclusion in Sec. 8.

2 Effective Interactions for aQGCs

An effective Lagrangian can be constructed in a model independent way for the anomalous quartic couplings, assuming that new physics beyond the SM still keeps $SU(2)_L \otimes U(1)_Y$ gauge invariance. The Lagrangian can be expressed in non-linear or linear representation [15, 20]. Since a higgs boson has been discovered in LHC, it is more preferable to work in the linear context.

The lowest order genuine aQGC operators in linear representation are dimension-8(dim-8). There are three classes of such operators: operators containing only covariant derivative of the field $D_\mu \Phi$, operators containing $D_\mu \Phi$ and field strength, and operators containing only the field strength [35]. In our research, we choose to study the below three dim-8 operators:

$$\mathcal{L}_{S0} = \frac{f_{S0}}{\Lambda^4} [(D_\mu \Phi)^\dagger D_\nu \Phi] \times [(D^\mu \Phi)^\dagger D^\nu \Phi], \quad (2.1)$$

$$\mathcal{L}_{S1} = \frac{f_{S1}}{\Lambda^4} [(D_\mu \Phi)^\dagger D^\mu \Phi] \times [(D_\nu \Phi)^\dagger D^\nu \Phi], \quad (2.2)$$

$$\mathcal{L}_{T0} = \frac{f_{T0}}{\Lambda^4} \text{Tr}[\hat{W}_{\mu\nu} \hat{W}^{\mu\nu}] \times \text{Tr}[\hat{W}_{\alpha\beta} \hat{W}^{\alpha\beta}], \quad (2.3)$$

where $f_{S0, S1, T0}$ represents the dimensionless numerical coefficients. Λ is a mass-dimension parameter associated with the energy scale of the new degrees of freedom.

One should note that the effective Lagrangian leads to tree-level unitarity violation at corresponding high energy. Usually, one can adjust the rising cross section by introducing an appropriate form factor. However, the choice of form factor is arbitrary and can be disputable [38, 39]. In this paper, we just present our results with some typical form factor, following the commonly used formalism [16].

$$f_J \rightarrow \frac{f_J}{(1 + \hat{s}/\Lambda_{ff}^2)^n} \quad (2.4)$$

where f_J could be the f_{S0} , f_{S1} and f_{T0} , \hat{s} is the partonic center-of-mass energy, Λ_{ff} represents the form factor cutoff scale.

Figs. 1 shows the energy scale at which tree-level unitarity would be violated without a form factor ($\Lambda_{ff} \rightarrow 0$) and the form factor scale (Λ_{ff}) that ensures tree-level unitarity up to the given energy. The region below the red line is unitarity safe. These bounds are estimated by using the form factor tool available with VBFNLO[37]. The form factor is determined by calculating on-shell vector bosons scattering and computing the zeroth partial wave of the amplitude. As unitarity criterion the absolute value of the real part of the zeroth partial wave has to be below 0.5.

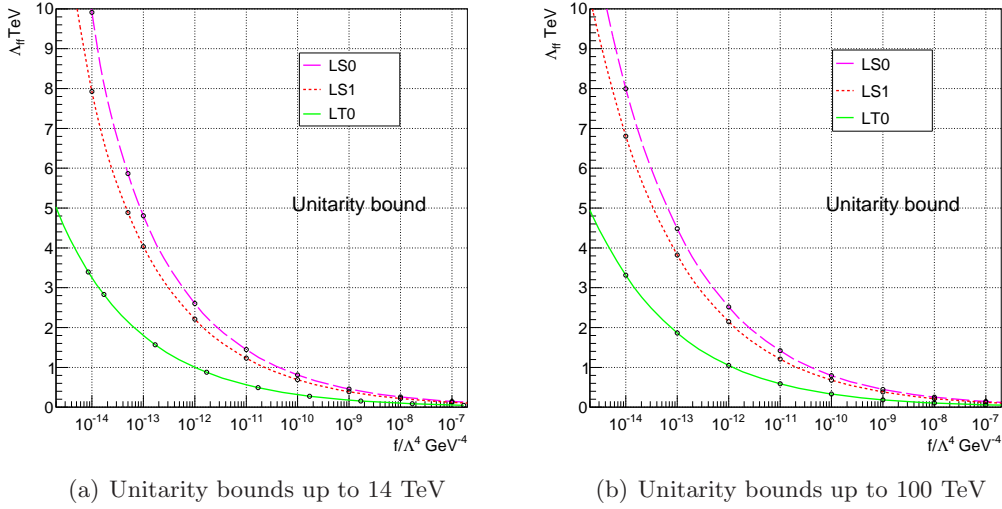


Figure 1. Unitarity bounds on form factor scale Λ_{ff} for different operators, got from $2 \rightarrow 2$ di-boson scattering for energy up to 14 and 100 TeV for $n = 2$. Unitarity safe region is below the curves.

3 Standard model $W^\pm W^\pm W^\mp$ production in pure leptonic decay channel

The MC simulations are carried out within MADGRAPH/MADEVENT v5[40]. The effective Lagrangian of $WWWW$ aQGCs are incorporated in MADGRAPH based on the FEYNRULES-UFO-ALOHA[42–44] framework. The signal and background processes are first generated at parton level by MADGRAPH [40] and MADEVENT [41], and then passed through the interface to PYTHIA 6 [45] for parton shower and hadronization. The detector simulations are done by using DELPHES 3.0 package [46], where we focus on CMS detector at the 8 and 14 TeV LHC and a combined ATLAS-CMS detector [47] at the future 100 TeV proton-proton collider. Finally, all events are delivered to EXROOTANALYSIS [48] and analyzed with ROOT [49]. In the analysis step, we use both traditional cut-based method and Multivariate Analysis(MVA) boosted decision tree(BDT) method [50]. The MVA BDT method is carried out under the TMVA package [51] included in ROOT.

The characteristic signal of this channel contains three well-defined leptons with total electric charge ± 1 , in association with large missing transverse energy \cancel{E}_T . Some example Feynman diagrams are plotted in Fig. 4, for $W^\pm W^\pm W^\mp$ production at the LHC, in the tripletonic final state $LL\bar{L}\nu$, with $l, L, \bar{L} = e, \mu$ and τ . Note that τ decays into e, μ at the ratio of about 35% and is handled by TAUOLA [52]. Fig. 2(a) involves TGCs and Fig. 2(c) involves higgs coupling, both are not sensitive to aQGC.

Five main backgrounds are taken into account: WZ (including virtual photon contributions), $t\bar{t}W$, ZZ , $t\bar{t}Z$ and WWZ , where WZ and $t\bar{t}W$ are dominant. Notice that the 4 leptons final state can be possible backgrounds with one lepton unidentified.

In order to improve event generating efficiency, we choose the following pre-selection cuts to generate unweighted events at parton level with MADGRAPH/MADEVENT .

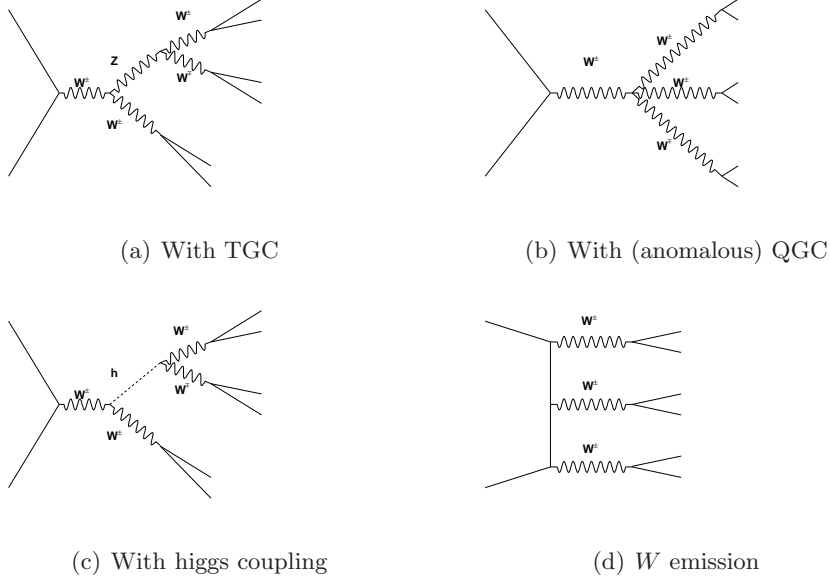


Figure 2. Example Feynman diagrams contributing to WWW productions at the LHC

- (1) $P_{Tl,j} \geq 10$ GeV,
- (2) $\cancel{E}_T \geq 20$ GeV,
- (3) $|\eta_j| < 5, |\eta_l| < 2.5$,
- (4) $R_{jj} > 0.4, R_{ll} > 0.3, R_{jl} > 0.3$,

where $R \equiv \sqrt{\Delta\phi^2 + \Delta\eta^2}$ in which ϕ being the azimuthal angle and η the pseudo-rapidity of a particle. For those backgrounds containing unidentified leptons, we do not apply any of the above cuts on leptons in order not to make bias.

Meanwhile, in the hard process generation with MADGRAPH/MADEVENT we adopt the CTEQ6L1 parton distribution functions (PDFs) [53] and set the renormalization and factorization scales as default dynamic scales.

In DELPHES, we consider no pileup and mean 20 pileup scenarios at 8 TeV LHC, no pileup, pileup 50 and 140 at 14 TeV LHC, and 50 and 140 pileup at future 100 TeV proton-proton collider.

As mentioned before, we present both cut-based method and BDT method to evaluate the feasibility of observing WWW production.

3.1 Cut-based method

In the cut-based analysis step, we apply the following high level cuts:

- (1) In order to select signal-like events, we require 3 and only 3 leptons in one event, the sum of electric charge of 3 leptons should be 1 or -1, and leading lepton $P_{Tl} > 35$ GeV, the rest two leptons' $P_{Tl} > 20$ GeV,

- (2) $\cancel{E}_T > 25$ GeV,
- (3) In order to suppress top quark related backgrounds, we exclude events with b-tagged jet,
- (4) To reject virtual photon production and leptons from hadron decay, we require the invariant mass of lepton pair $m_{ll} > 12$ GeV,
- (5) The transverse mass of 3 lepton system $m_T > 300$ GeV,
- (6) $R_{ll} > 0.5$.

We present our analysis in two schemes.

- *scheme 1* (s1): We require at least one pair of opposite-sign same-flavor(OSSF) leptons and its mass m_{OSSF} satisfied $|m_{OSSF} - M_Z| > 15$ GeV,
- *scheme 2* (s2): We only collect events from the remaining lepton topologies: $e^-\mu^+\mu^+$, $e^+\mu^-\mu^-$, $\mu^-e^+e^+$, and $\mu^+e^-e^-$. These final states topologies only occur in triple W boson production related samples.

Scheme 2 is to further suppress the backgrounds with Z boson leptonic decay.

3.2 Multivariate analysis BDT method

In our research, we use MVA classification to study the feasibility of $W^\pm W^\pm W^\mp$ production. A typical MVA classification analysis consists of two independent phases: the training phase, where the MVA methods are trained, tested and evaluated, and application phase, where the methods are applied to the concrete classification problem they have been trained for.

Before going into training phase, we preselect the events with the preselection cuts:

- (1) 3 and only 3 leptons in one event, the sum of electric charge of 3 leptons should be 1 or -1,
- (2) $\cancel{E}_T > 25$ GeV,
- (3) Exclude events with b-tagged jet,
- (4) the mass of arbitrary two leptons $m_{ll} > 12$ GeV,
- (5) R_{ll} is larger than 0.5.

After preselection, we input the following discriminating variables to the TMVA package: 3 lepton's P_{Tl} , η_l , R_{ll} , transverse missing energy, transverse mass of 3 leptons m_T , H_T , M_{ll} , P_{Tll} , and the m_{ll} of the lepton pair with m_{ll} closest to M_Z . These variables would be used for MVA training.

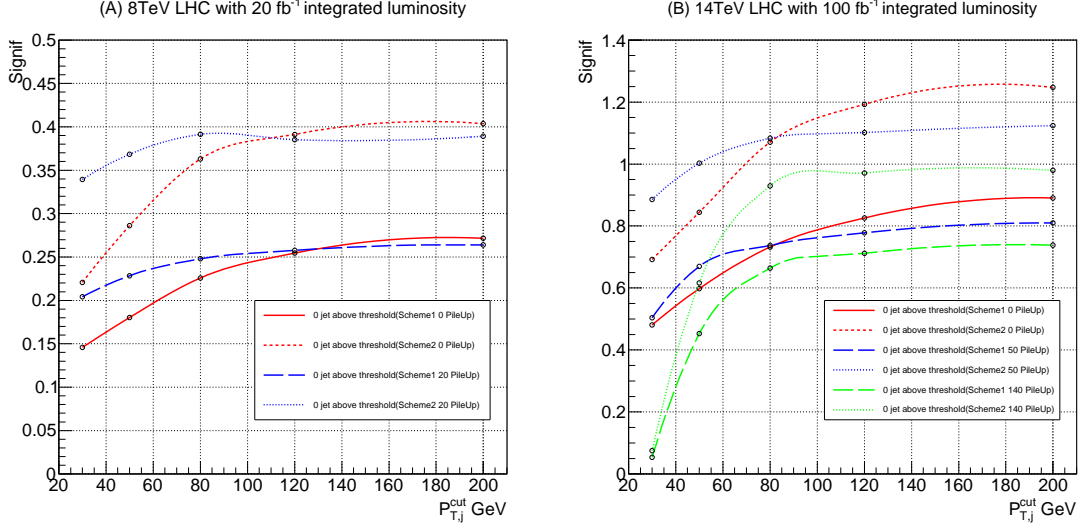


Figure 3. WW production in pure leptonic decay significances, varying jet reconstructing cut P_{Tj}^{cut} .

3.3 Numerical Results

What we are interested in is evaluating the feasibility of observing triple gauge boson $W^\pm W^\pm W^\mp$ Production. To optimize the results, we introduce a further requirement $P_{Tj} > P_{Tj}^{cut}$ and $n_j = 0$ in addition to all the cuts mentioned above in cut-based analysis, where P_{Tj}^{cut} is the jet reconstructing cut and n_j is reconstructed jet number. The purpose of setting this special cut is to suppress more top-quark related background and keeping high signal efficiency at the same time. Compared with the signal process, $t\bar{t}W$ and $t\bar{t}Z$ tend to radiate more jets. Furthermore, the hard physics scale is higher and thus one or more jets can be harder than the jets in signal.

The significances are shown in Fig. 3, calculated with Eq. (3.1). It is interesting to note that when P_{Tj}^{cut} is getting larger, the significance goes higher. This means the cases of no requirement of jet P_T have the largest significances (which comes from the statistic increasing). Thus we are not going to apply any jet veto in the following.

We list the 8 TeV event numbers for the signal and backgrounds and significances in Table. 1 and 14 TeV in Table. 2. A significance about $0.28 \sim 0.41\sigma$ can be achieved to observe $W^\pm W^\pm W^\mp$ production in pure leptonic decay channel at 8 TeV LHC and $0.75 \sim 1.28\sigma$ at 14 TeV LHC. We note that Scheme 2 tends to have larger significance than Scheme 1, due to further suppression on WZ background. The results of the two scheme can be combined in future experimental studies. Moreover, the BDT method can gives us some gain but not much.

$$Signif = \sqrt{2\ln(Q)}, Q = (1 + N_s/N_b)^{N_{obs}} \exp(-N_s). \quad (3.1)$$

Processes	Cross section[fb]	Events				
		cut-based				BDT
		Pileup 0		Pileup 20		Pileup 0
		s1	s2	s1	s2	s1
WWW	1.06	2.08	0.636	2.03	0.612	1.99
WZ	235	47.3	0.800	45.7	0.925	38.0
$t\bar{t}W$	3.97	2.81	0.859	2.96	0.935	4.84
ZZ	129	3.97	0.206	7.95	0.155	2.94
$t\bar{t}Z$	1.41	0.521	0.146	0.541	0.147	0.958
WWZ	0.358	0.344	0.0983	0.334	0.0936	0.320
significance		0.279	0.418	0.266	0.391	0.288

Table 1. Event numbers and significances of WWW production in pure leptonic decay channel at the LHC with $\sqrt{s} = 8$ TeV and integrated luminosity of 20 fb^{-1} .

Processes	Cross section[fb]	Events						
		cut-based						BDT
		Pileup 0		Pileup 50		Pileup 140		Pileup 0
		s1	s2	s1	s2	s1	s2	s1
WWW	2.17	21.0	6.29	20.0	5.82	17.9	5.18	20.2
WZ	412	421	6.86	429	6.72	398	6.59	337
$t\bar{t}W$	9.88	33.4	10.3	38.2	11.5	38.8	11.9	56.0
ZZ	273	40.4	1.09	98.8	1.64	107	2.73	32.7
$t\bar{t}Z$	6.35	10.8	2.78	12.6	3.46	13.3	3.60	18.5
WWZ	0.849	3.73	1.04	3.73	1.01	3.54	0.949	3.23
significance		0.922	1.28	0.822	1.14	0.751	0.989	0.946

Table 2. Event numbers and significances of WWW production in pure leptonic decay channel at the LHC with $\sqrt{s} = 14$ TeV and integrated luminosity of 100 fb^{-1} .

4 Standard model $W^{\pm}W^{\pm}W^{\mp}$ production in semileptonic decay channel

In semileptonic decay channel analysis, we use exactly the same simulation framework as in pure leptonic decay channel in Sec 3. We only consider the most significant case $l^{\pm}\nu l^{\pm}\nu jj$ final state here. The same sign leptons come from the two same sign W bosons decay. The other opposite charge W boson decays hadronically into two jets. Here three main categories of background processes contribute to this channel:

- $W^{\pm}W^{\pm}jj$ decaying to $l^{\pm}\nu l^{\pm}\nu jj$ where the two jets don't come from an on-shell W boson. Both electroweak process and QCD process are included,
- $WZjj$ decaying to $l^{\pm}\nu l^{\pm}l^{\mp}jj$, where one of the leptons is missing. Both electroweak process and QCD process are included,

- $t\bar{t}W$, all decay modes are included.

When generating events at MADGRAPH, we apply the following preselection cuts.

- (1) $P_{T,j} \geq 20$ GeV, $P_{T,l} \geq 10$ GeV.
- (2) $\cancel{E}_T \geq 10$ GeV.
- (3) $|\eta_j| < 5$, $|\eta_l| < 2.5$.
- (4) $R_{jj} > 0.4$, $R_{ll} > 0.4$, $R_{jl} > 0.4$.

Note that Backgrounds containing unidentified leptons don't have cuts related to leptons applied on.

4.1 Cut-based method

In the cut-based analysis step, the optimized event selection is shown in Table. 3, where N_{lep} is the number of lepton that has $P_T > 20$ GeV and $|\eta| \leq 2.4$, $N_{\text{lep}}^{\text{loose}}$ is the number of lepton that has $P_T > 10$ GeV and $|\eta| \leq 2.4$, N_{jet} is the number of jet that has $P_T > 30$ GeV and $|\eta| \leq 5$, m_{jj} is the invariant mass of the leading two jets and m_W is mass of W boson.

	8 TeV		14 TeV	
Pileup	20	0	50	140
N_{lep}			$= 2$	
$N_{\text{lep}}^{\text{loose}}$			$= 2$	
lepton sign		$(+, +)$ or $(-, -)$		
\cancel{E}_T		$\geq 30 \text{ GeV}$		
N_{jet}	$= 2$	$= 2$	$\geq 2, \leq 3$	≥ 2
$ m_{jj} - m_W $	$\leq 15 \text{ GeV}$	$\leq 15 \text{ GeV}$	$\leq 20 \text{ GeV}$	$\leq 30 \text{ GeV}$

Table 3. $l^\pm \nu l^\pm \nu jj$ Event selections, for N_{jet} and m_{jj} optimization check also Figures. 4(a) and 4(b).

4.2 Multivariate analysis BDT method

The event preselections before going into training phase of BDT are shown as below:

- (1) The event contains two and only two reconstructed leptons with $P_T > 20$ GeV and $|\eta| < 2.4$. Events with extra lepton whose $P_T > 10$ GeV and $|\eta| < 2.4$ are vetoed,
- (2) $\cancel{E}_T > 30$ GeV,
- (3) At least 2 jets, whose $P_{T,j} \geq 30$ GeV, $|\eta| \leq 5$.

The following discriminate variables will be put into TMVA packages: P_{Tj} , η_j , m_j , N_{jet} , leading lepton P_T , \cancel{E}_T , the invariant mass of two leading jets m_{jj} , distance between the leading two jets R_{jj} , the azimuthal angle between two leading jets $\Delta\phi_{jj}$, lepton pair's P_T ,

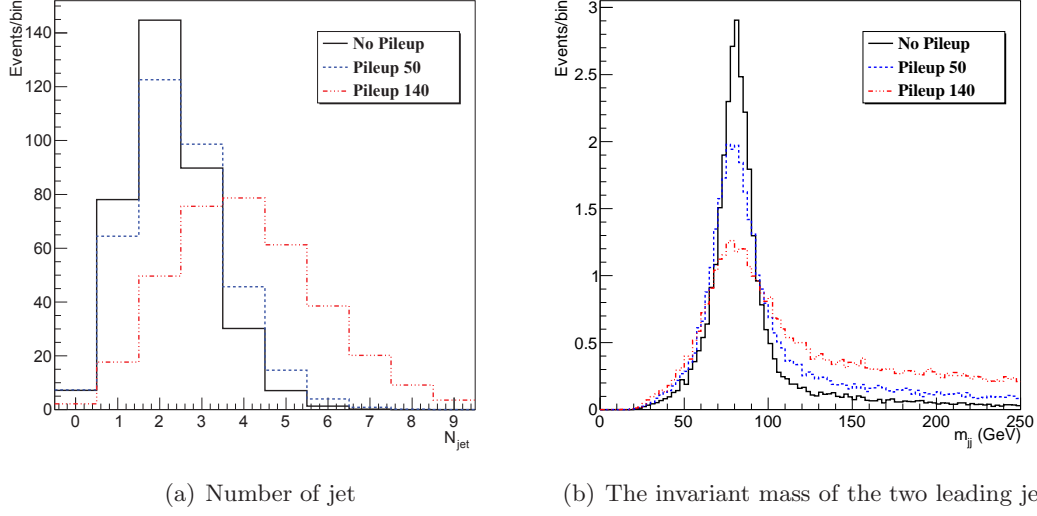


Figure 4. Distribution of signal process $l^\pm\nu l^\pm\nu jj$ in different pileup scenarios at 14 TeV LHC

R_{ll} , the azimuthal angle between two leptons $\Delta\phi_{ll}$, the azimuthal angle between \cancel{E}_T and the lepton pair $\Delta\phi_{ll, \cancel{E}_T}$, the minimum of the azimuthal angles between lepton and \cancel{E}_T $\Delta\phi_{l, \cancel{E}_T}^{min}$ and the minimum distance between the leading jet and lepton R_{jl}^{min} .

4.3 Numerical results

Table. 4 shows the 8 TeV event numbers for the signal and backgrounds and significances and 14 TeV in Table. 5. A significance of 0.5σ can be reached to observe the $W^\pm W^\pm W^\mp$ production in semileptonic decay channel at 8 TeV LHC and $0.91 \sim 1.96\sigma$ at 14 TeV. As shown in the Table. 5, with the pileup increasing, the significance drops rapidly when using cut-based method. It mainly dues to the pileup jets which result in worse jet energy resolution. Fig. 4(a) shows the jet number distribution from different pileup scenarios. Jet number increases with pileup. Especially, in 140 pileup scenario, most of events contain at least 4 jets, this would make the N_{jet} cut has less efficiency to separate signal from backgrounds. Similarly, in Fig. 4(b), the invariant mass of two leading jets m_{jj} distribution has a broader peak near W boson mass and harder tail in 140 pileup case. This would also reduce the discrimination between signal and backgrounds. In general, unlike the pure leptonic decay channel case, the significance of observing the WWW production in semileptonic channel suffers more contamination from pileup event because it is difficult to identify the jet's original source, whether it come from signal or pileup.

5 Anomalous $WWWW$ Couplings

5.1 aQGC in pure leptonic decay channel

The $W^\pm W^\pm W^\mp$ production can be sensitive to aQGC $WWWW$. The cross sections, via MADGRAPH/MADEVENT after preselection cuts mentioned in Sec. 3, can grow quickly with

Processes	Cross section[fb]	Events	
		cut-based	BDT
WWW	1.732	1.9	1.7
$t\bar{t}W$	169.7	1.7	1.6
$WWjj$	19.95	3.2	2.9
$WZjj$	192.3	8.4	4.9
Significance		0.51	0.54

Table 4. Event numbers and significances of WWW production in semileptonic decay channel at the LHC with $\sqrt{s} = 8$ TeV in mean pileup 20 scenario with integrated luminosity of 20 fb^{-1} .

Processes	Cross section[fb]	Events					
		Pileup 0		Pileup 50		Pileup 140	
		cut-based	BDT	cut-based	BDT	cut-based	BDT
WWW	3.586	22.1	21.9	22	20.7	21.2	39.7
$t\bar{t}W$	480.2	14.4	19.7	53.2	36.5	112.6	140.2
$WWjj$	49.15	13.3	15.5	24.4	27.9	46.7	121.8
$WZjj$	627.9	106.7	82.9	212.7	138.8	379.5	680
Significance		1.86	1.96	1.28	1.43	0.91	1.28

Table 5. Event numbers and significances of WWW production in semileptonic decay channel at the LHC with $\sqrt{s} = 14$ TeV with integrated luminosity of 100 fb^{-1} .

the increase of the absolute values of aQGCs, as demonstrated in Fig. 5. Furthermore, as shown in Fig. 6, the aQGCs lead to excesses on the hard tails in various kinematic region. Thus we refine the cuts in both schemes in Sec. 3 to enhance the sensitivity of QGCs without form factor as following, e.g.:

- (1) $\cancel{E}_T > 350$ GeV,
- (2) The transverse mass of 3 leptons $m_T > 1$ TeV,
- (3) leading lepton $P_T > 200$ GeV.

For the form factor case, \cancel{E}_T and leptons would be softer, thus we refine our cuts as:

- (1) $\cancel{E}_T > 80$ GeV,
- (2) The transverse mass of 3 leptons $m_T > 250$ GeV,
- (3) leading lepton $P_T > 50$ GeV.

After all these selection cuts, the significances are calculated and displayed as following as functions of the QGCs f_{S0} , f_{S1} and f_{T0} , at the 8 TeV LHC with an integrated luminosity of 20 fb^{-1} and 14 TeV LHC with an integrated luminosity of 100 fb^{-1} , respectively. As shown in Ref. [36], pileup would not affect aQGC measurement at hard kinematic region, thus we produce aQGC samples without pileup mixing. As mentioned in sec. 3, we category

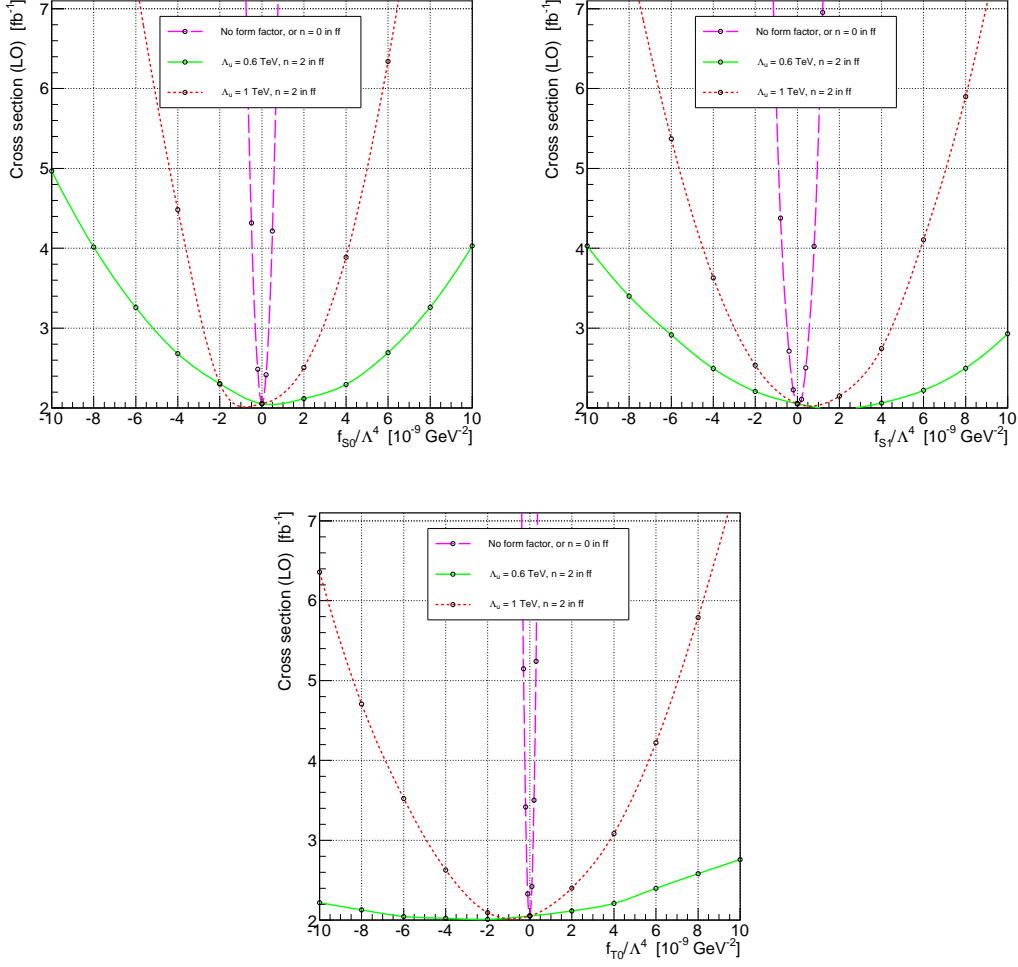


Figure 5. Cross section dependences on $WWWW$ anomalous couplings $f_{S0,S1}/\Lambda^4$ and f_{T0}/Λ^4 at 14 TeV LHC with different form factors applied.

2 different analysis schemes, but only the more stringent results (Scheme 2) are presented here. The results of 8 TeV LHC and 14 TeV LHC are shown in Table. 6 and Table. 7, both with/without form factor results are shown. Compared with the Fig. 1, for 8 TeV results, even with form factors applied, the aQGC limits are unitarity unsafe. But for 14 TeV results, they are close to unitarity safe region.

5.2 aQGC in semileptonic decay channel

After generating event and applying preselection cuts mentioned in Sec. 4, some distributions of WW production and aQGC of $f_{S0}/\Lambda^4 = 6 \times 10^{-10}$ GeV at 14 TeV LHC are shown in Fig. 7. The aQGC has more excess at hard tail. Based on this characteristic, to further improve the sensitivity on aQGC, we refine the cuts in addition to those cuts in Sec. 4:

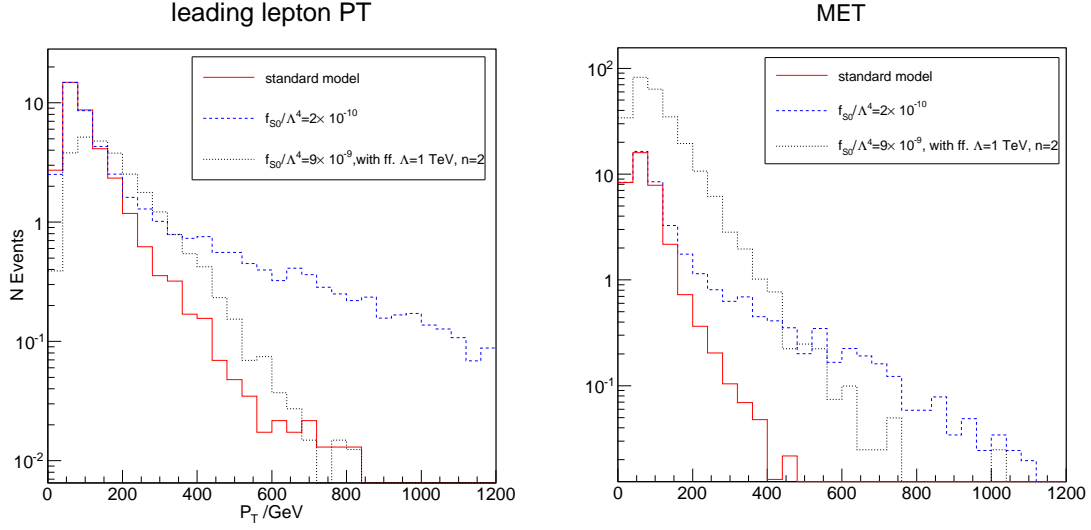


Figure 6. The leading lepton P_T and \cancel{E}_T distributions for $W^\pm W^\pm W^\mp$ productions at 14 TeV LHC, with or without aQGCs and form factor.

	No form factor		$\Lambda = 1 \text{ TeV}, n=2$	
	lower limit	upper limit	lower limit	upper limit
$\frac{f_{S0}}{\Lambda^4}$	-1.32×10^{-9}	1.30×10^{-9}	-8.74×10^{-9}	8.87×10^{-9}
$\frac{f_{S1}}{\Lambda^4}$	-2.00×10^{-9}	2.03×10^{-9}	-1.08×10^{-8}	1.17×10^{-8}
$\frac{f_{T0}}{\Lambda^4}$	-5.56×10^{-12}	5.44×10^{-12}	-1.30×10^{-10}	1.21×10^{-10}

Table 6. Constraints on anomalous quartic couplings parameters f_{S0}/Λ^4 , f_{S1}/Λ^4 and f_{T0}/Λ^4 at 8 TeV LHC via WWW production pure leptonic decay channel with integrated luminosity of 20 fb^{-1} . Units are in GeV^{-4} .

	No form factor		$\Lambda = 1 \text{ TeV}, n=2$		$\Lambda = 0.5 \text{ TeV}, n=2$	
	lower limit	upper limit	lower limit	upper limit	lower limit	upper limit
$\frac{f_{S0}}{\Lambda^4}$	-1.78×10^{-10}	1.79×10^{-10}	-2.80×10^{-9}	3.08×10^{-9}	-1.21×10^{-8}	1.29×10^{-8}
$\frac{f_{S1}}{\Lambda^4}$	-2.66×10^{-10}	2.78×10^{-10}	-3.47×10^{-9}	4.44×10^{-9}	-1.29×10^{-8}	1.81×10^{-8}
$\frac{f_{T0}}{\Lambda^4}$	-5.80×10^{-13}	5.87×10^{-13}	-4.48×10^{-11}	3.46×10^{-11}	-2.46×10^{-10}	1.76×10^{-10}

Table 7. Constraints on anomalous quartic couplings parameters f_{S0}/Λ^4 , f_{S1}/Λ^4 and f_{T0}/Λ^4 at 14 TeV LHC via WWW production pure leptonic decay channel with integrated luminosity of 100 fb^{-1} . Units are in GeV^{-4} .

- (1) The invariant mass of the same sign lepton pair plus two leading jets $m_{lljj} \geq 600$ GeV,
- (2) $\cancel{E}_T > 150$ GeV.

For the form factor case, \cancel{E}_T and jets would be softer, thus we refine our cuts as:

- (1) The invariant mass of the same sign lepton pair plus two leading jets $m_{lljj} \geq 200$ GeV,

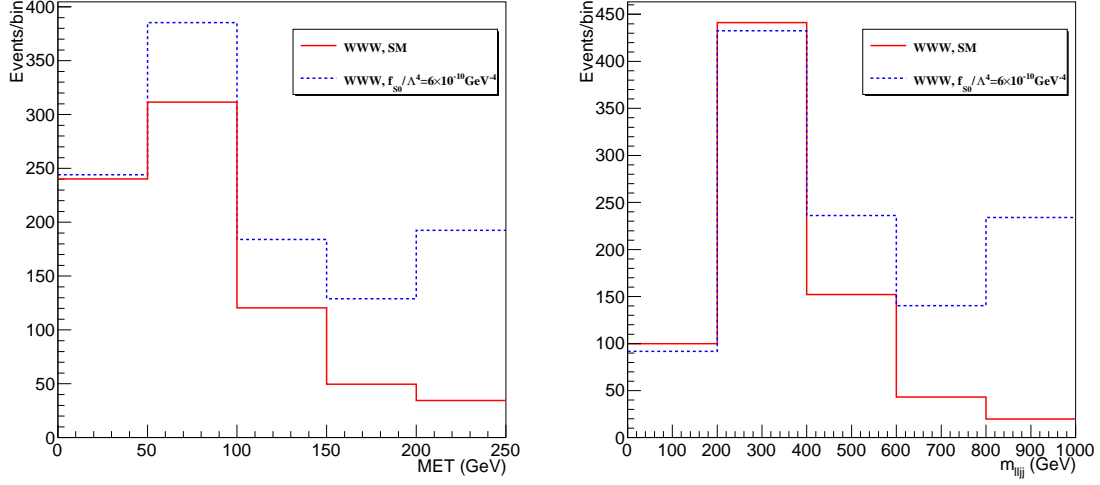


Figure 7. The in \cancel{E}_T and m_{ljj} distributions for $W^\pm W^\pm W^\mp$ productions at 14 TeV LHC, with the aQGCs $f_{S0}/\Lambda^4 = 6 \times 10^{-10} \text{GeV}^{-4}$. No form factor is applied here. The last bin includes overflow.

- (2) $\cancel{E}_T > 50 \text{ GeV}$.

The aQGC limits for 14 TeV LHC are given in Table. 8, via WWW production semileptonic decay channel with integrated luminosity of 100 fb^{-1} , with/without form factor.

One can also compare our results with the previous MC simulation given by Snowmass Collaboration [36] and O. Eboli et.al. based on vector boson fusion(VBF) [35], respectively, as shown in Table 9. The semileptonic channel results still suffer from bad jet energy resolution. But in pure leptonic channel, due to the optimized selection, we set a more stringent limit on f_{T0}/Λ^4 , $8 \times 10^{-13} \text{GeV}^{-4}$ in 5σ with 100 fb^{-1} . This result is better than Snowmass one. As to the weak boson fusion, however, our $W^\pm W^\pm W^\mp$ channel seems to set looser limits on QGCs. However, triple W production channel has simpler event topology and populates at different kinematic phase space, thus can present us more information other than VBF channel.

	No form factor		$\Lambda = 1 \text{ TeV}, n=2$		$\Lambda = 0.5 \text{ TeV}, n=2$	
	lower limit	upper limit	lower limit	upper limit	lower limit	upper limit
$\frac{f_{S0}}{\Lambda^4}$	-4.56×10^{-10}	4.58×10^{-10}	-3.08×10^{-9}	3.39×10^{-9}	-1.20×10^{-8}	1.40×10^{-8}
$\frac{f_{S1}}{\Lambda^4}$	-9.46×10^{-10}	9.85×10^{-10}	-4.00×10^{-9}	5.26×10^{-9}	-1.28×10^{-8}	1.77×10^{-8}
$\frac{f_{T0}}{\Lambda^4}$	-2.80×10^{-12}	2.70×10^{-12}	-7.60×10^{-11}	6.00×10^{-11}	-4.03×10^{-10}	2.88×10^{-10}

Table 8. Constraints on anomalous quartic couplings parameters f_{S0}/Λ^4 , f_{S1}/Λ^4 and f_{T0}/Λ^4 at 14 TeV LHC via WWW production semileptonic decay channel with integrated luminosity of 100 fb^{-1} . Units are in GeV^{-4} .

	WWW in p.l decay 95% CL with 100 fb ⁻¹		WWW in s.l decay 95% CL with 100 fb ⁻¹		VBF WW 99% CL with 100 fb ⁻¹		Snowmass WWW 5σ with 300 fb ⁻¹	
	lower limit	upper limit	lower limit	upper limit	lower limit	upper limit	lower limit	upper limit
$\frac{I_{sp}}{\Lambda^4}$	-1.8×10^{-10}	1.8×10^{-10}	-4.6×10^{-10}	4.6×10^{-10}	-2.2×10^{-11}	2.4×10^{-11}	-	-
$\frac{I_{s1}}{\Lambda^4}$	-2.7×10^{-10}	2.8×10^{-10}	-9.5×10^{-10}	9.9×10^{-10}	-2.5×10^{-11}	2.5×10^{-11}	-	-
$\frac{I_{T0}}{\Lambda^4}$	-5.8×10^{-13}	5.9×10^{-13}	-2.8×10^{-12}	2.7×10^{-12}	-	-	-	1.2×10^{-12}

Table 9. Constraints on aQGC parameter limit comparison to previous MC study at 14 TeV LHC. All without form factor applied. Units are in GeV⁻⁴.

6 WWW production and aQGC at 100 TeV future pp collider

We also studied WWW production and aQGCs at 100 TeV future proton-proton collider. The simulation framework is basically the same as in 8 TeV and 14 TeV LHC study. However, at the level of detector fast simulation, we use the Snowmass combined LHC detector which is a hybrid of CMS and ATLAS detectors [47], using the tracker components from CMS and calorimeter from ATLAS, etc. Effects of average 50 and 140 pileup scenarios will be considered here.

6.1 Pure leptonic decay channel

For SM $W^\pm W^\pm W^\mp$ production and aQGC in pure leptonic decay, event selection cuts are the same as the studies of LHC in Sec. 3 and 5. The event numbers for the signal, backgrounds and significances are listed in Table. 10. One can see that it reaches a significance of $10 \sim 14\sigma$ to observe SM $W^\pm W^\pm W^\mp$ production at 100 TeV future proton-proton collider with 3000 fb⁻¹ integrated luminosity.

Processes	Cross section[fb]	Events			
		cut-based			
		Pileup 50		Pileup 140	
		s1	s2	s1	s2
WWW	15.6	4758	1416	3855	1156
WZ	2570	92185	1670	82060	1696
t \bar{t} W	89.7	8607	2539	9930	3211
ZZ	2674	26633	481	24226	1283
t \bar{t} Z	454	15240	4408	18180	5034
WWZ	14.1	1164	317	993	255
Significance		12.5	14.6	10.5	10.8

Table 10. Event numbers and significances of WWW production in pure leptonic decay channel at future proton-proton collider with $\sqrt{s} = 100$ TeV and integrated luminosity of 3000 fb⁻¹.

6.2 Semileptonic decay channel

Unlike the LHC, in 100 TeV proton proton collider, the pileup contamination in semileptonic channel is more severe. Therefore, we optimise the event selection cuts again (most of

them are related to jets)(See table. 11). We only consider those jet in the tracker region, namely, $|\eta| \leq 2.5$. For this, we define N_{jet}^{tight} as the number of jets which satisfy $p_T \geq 30$ GeV and $|\eta| \leq 2.5$. The results are shown in Table. 12. It reaches $10 \sim 16\sigma$ to observe the SM $W^\pm W^\pm W^\mp$ production.

Pileup	50	140
N_{lep}	$= 2$	
Sign	$(+, +)$ or $(-, -)$	
\cancel{E}_T	≥ 30 GeV	
N_{jet}^{tight}	$\geq 2, \leq 4$	≥ 2
$ m_{jj} - m_W $	≤ 25 GeV	≤ 40 GeV

Table 11. $l^\pm \nu l^\pm \nu jj$ Event selections at 100 TeV proton proton collider

Processes	Cross section[fb]	Events			
		Pileup 50		Pileup 140	
		cut-based	BDT	cut-based	BDT
WWW	26	6465	12156	7794	13485
$t\bar{t}W$	7684	35961	65928	60396	100047
$WWjj$	535	30507	41124	71610	75708
$WZjj$	16250	209820	437775	429195	693225
Significance		12.3	16.4	10.4	14.4

Table 12. Event numbers and significances of WWW production in semileptonic decay channel at future proton-proton collider with $\sqrt{s} = 100$ TeV and integrated luminosity of 3000 fb^{-1} .

6.3 Anomalous quartic couplings

We also wish to explore the potential of probing aQGC at 100 TeV collider. The event selections of aQGC is basically the same as in Sec. 5. We list the results of both pure leptonic and semileptonic channel in Table. 13 and Table. 14

	No form factor		$\Lambda = 1 \text{ TeV, n=2}$		$\Lambda = 0.5 \text{ TeV, n=2}$	
	lower limit	upper limit	lower limit	upper limit	lower limit	upper limit
$\frac{f_{S0}}{\Lambda^4}$	-2.93×10^{-12}	3.04×10^{-12}	-1.65×10^{-9}	1.50×10^{-9}	-2.06×10^{-8}	2.15×10^{-8}
$\frac{f_{S1}}{\Lambda^4}$	-1.30×10^{-12}	1.16×10^{-12}	-1.87×10^{-9}	2.37×10^{-9}	-2.75×10^{-8}	2.84×10^{-8}
$\frac{f_{T0}}{\Lambda^4}$	-3.69×10^{-15}	2.97×10^{-15}	-9.18×10^{-12}	6.76×10^{-12}	-9.90×10^{-11}	7.30×10^{-11}

Table 13. Constraints on anomalous quartic couplings parameters f_{S0}/Λ^4 , f_{S1}/Λ^4 and f_{T0}/Λ^4 at 100 TeV future proton proton collider via WWW production pure leptonic decay channel with integrated luminosity of 3000 fb^{-1} . Units are in GeV^{-4} .

	No form factor		$\Lambda = 1 \text{ TeV}, n=2$		$\Lambda = 0.5 \text{ TeV}, n=2$	
	lower limit	upper limit	lower limit	upper limit	lower limit	upper limit
$\frac{f_{S0}}{\Lambda^4}$	-1.03×10^{-10}	1.00×10^{-10}	-8.79×10^{-10}	1.17×10^{-9}	-2.99×10^{-9}	5.18×10^{-9}
$\frac{f_{S1}}{\Lambda^4}$	-1.93×10^{-10}	2.21×10^{-10}	-1.08×10^{-9}	2.27×10^{-9}	-3.26×10^{-9}	7.59×10^{-9}
$\frac{f_{T0}}{\Lambda^4}$	-2.00×10^{-13}	2.00×10^{-13}	-3.10×10^{-11}	1.60×10^{-11}	-1.84×10^{-10}	6.80×10^{-11}

Table 14. Constraints on anomalous quartic couplings parameters f_{S0}/Λ^4 , f_{S1}/Λ^4 and f_{T0}/Λ^4 at 100 TeV proton proton collider via WWW production semileptonic decay channel with integrated luminosity of 3000 fb^{-1} . Units are in GeV^{-4} .

7 Unitarity safety discussion

In the previous study, besides no form factor case, we exploit also form factors with $\Lambda_{ff} = 0.5/1 \text{ TeV}$ and $n = 2 \text{ TeV}$. As for both 14 and 100 TeV future collider, by comparing Tables. 7, 8, 13, 14 with Fig. 1, one can see that applying those form factors will not yet lead to unitarity safe, due to lack of luminosity. We provide the needed luminosity (estimated based on our analysis in Sec. 6.3 to reach unitarity safety in Tables. 15 and 16. In general, it needs very high luminosity to reach safe unitarity. Same situation appears in the 8TeV CMS $WV\gamma$ measurement [30] which finds that the unitarity safety can not be satisfied with a dipole form factor, however, "unitarity conserving new physics with a structure more complex than that represented by a dipole form factor is possible" [30] .

aQGC, $\Lambda = 1 \text{ TeV}, n=2$	Required Luminosity(fb^{-1})
$\frac{f_{S0}}{\Lambda^4} = 4 \times 10^{-11}$	16000
$\frac{f_{S1}}{\Lambda^4} = 1 \times 10^{-11}$	19000
$\frac{f_{T0}}{\Lambda^4} = 1 \times 10^{-12}$	4500

Table 15. The unitarity safe aQCG boundary (from Fig. 1) and corresponding required luminosity to reach it, for 14TeV future collider, with form factor $\Lambda = 1 \text{ TeV}$ and $n = 2$

aQGC, $\Lambda = 0.5 \text{ TeV}, n=2$	Required Luminosity(fb^{-1})
$\frac{f_{S0}}{\Lambda^4} = 6 \times 10^{-10}$	6000
$\frac{f_{S1}}{\Lambda^4} = 3 \times 10^{-10}$	12000
$\frac{f_{T0}}{\Lambda^4} = 2 \times 10^{-11}$	4000

Table 16. The unitarity safe aQCG boundary (from Fig. 1) and corresponding required luminosity to reach it, for 14 TeV future collider, with form factor $\Lambda = 0.5 \text{ TeV}$ and $n = 2$

8 Conclusion

The future upgrade of LHC and the next generation 100 TeV proton-proton collider with higher center of mass energy and luminosity enable measurement of triple gauge boson production and anomalous quartic gauge couplings, and $W^\pm W^\pm W^\mp$ production will be

a potential process that can be exploited to test the SM predictions and probe $WWWW$ anomalous coupling exclusively with lower background contamination.

In summary, our study shows that at 8 TeV LHC with an integrated luminosity of 20 fb^{-1} , 14 TeV LHC with 100 fb^{-1} and 100 TeV next generation proton-proton collider with 3000 fb^{-1} , for pure(semi-) leptonic decay channel one can reach a significance of about 0.4(0.5), 1.2(2) and 10(14) σ to probe the SM $W^\pm W^\pm W^\mp$ production, and can constrain at 95% C.L. the anomalous $WWWW$ coupling parameters $f_{S0,S1}/\Lambda^4$ at $1 \times 10^{-9} \text{ GeV}^{-4}$ and f_{T0}/Λ^4 at $1 \times 10^{-12} \text{ GeV}^{-4}$ at 8 TeV LHC with 20 fb^{-1} , $f_{S0,S1}/\Lambda^4$ at $1 \times 10^{-10}(10^{-10}) \text{ GeV}^{-4}$ and f_{T0}/Λ^4 at $1 \times 10^{-13}(10^{-12}) \text{ GeV}^{-4}$ at 14 TeV LHC with 100 fb^{-1} and $f_{S0,S1}/\Lambda^4$ at $1 \times 10^{-12}(10^{-10}) \text{ GeV}^{-4}$ and f_{T0}/Λ^4 at $1 \times 10^{-15}(10^{-13}) \text{ GeV}^{-4}$ at 100 TeV with 3000 fb^{-1} . When the energy scale moving from 14 TeV to 100 TeV, the significance gain in pure leptonic channel is bigger than semileptonic channel, which may be due to that the QCD backgrounds increase much faster than the pure leptonic background.

Our limits on \mathcal{L}_S operators are presented for the first time in $W^\pm W^\pm W^\mp$ channel, although less tighter than the previous results from VBF process, however, triple W production channel populates at different kinematic phase space, thus can present us more information other than VBF channel. On the other hand, our limits on f_{T0}/Λ^4 are better than Snowmass due to optimized selection cuts. Moreover, it is the first time to study the $W^\pm W^\pm W^\mp$ production in semileptonic channel.

Acknowledgments

This work is supported in part by the National Natural Science Foundation of China, under Grants No. 11475180, , No. 10721063, No. 10975004, No. 10635030 and No. 11205008, and National Fund for Fostering Talents in Basic Science, under Grant No. J1103206.

References

- [1] F. Gianotti, CERN Seminar, Update on the Standard Model Higgs searches in ATLAS, July, 4 2012. ATLAS-CONF-2012-093
- [2] J. Incandela, CERN Seminar, Update on the Standard Model Higgs searches in CMS, July, 4 2012.
- [3] S. Chatrchyan *et al.* [CMS Collaboration], Phys. Lett. B **716**, 30 (2012) [arXiv:1207.7235 [hep-ex]].
- [4] G. Aad *et al.* [ATLAS Collaboration], Phys. Lett. B **716**, 1 (2012) [arXiv:1207.7214 [hep-ex]].
- [5] P. Achard *et al.* [L3 Collaboration], Phys. Lett. B **547**, 151 (2002) [hep-ex/0209015].
- [6] P. Abreu *et al.* [DELPHI Collaboration], Phys. Lett. B **502**, 9 (2001) [hep-ex/0102041].
- [7] TK. Gounder [CDF and D0 Collaborations], hep-ex/9903038.
- [8] B. Abbott *et al.* [D0 Collaboration], Phys. Rev. D **62**, 052005 (2000) [hep-ex/9912033].
- [9] G. Aad *et al.* [ATLAS Collaboration], Phys. Rev. Lett. **108**, 041804 (2012) [arXiv:1110.5016 [hep-ex]].

- [10] S. Chatrchyan *et al.* [CMS Collaboration], Eur. Phys. J. C **73**, 2283 (2013) [arXiv:1210.7544 [hep-ex]].
- [11] F. Campanario, V. Hankele, C. Oleari, S. Prestel and D. Zeppenfeld, Phys. Rev. D **78**, 094012 (2008) [arXiv:0809.0790 [hep-ph]].
- [12] G. Bozzi, F. Campanario, V. Hankele and D. Zeppenfeld, Phys. Rev. D **81**, 094030 (2010) [arXiv:0911.0438 [hep-ph]].
- [13] G. Bozzi, F. Campanario, M. Rauch and D. Zeppenfeld, Phys. Rev. D **83**, 114035 (2011) [arXiv:1103.4613 [hep-ph]].
- [14] G. Bozzi, F. Campanario, M. Rauch, H. Rzehak and D. Zeppenfeld, Phys. Lett. B **696** (2011) 380 [arXiv:1011.2206 [hep-ph]].
- [15] G. Belanger and F. Boudjema, Phys. Lett. B **288**, 201 (1992).
- [16] O. J. P. Eboli, M. C. Gonzalez-Garcia and S. M. Lietti, Phys. Rev. D **69**, 095005 (2004) [hep-ph/0310141].
- [17] O. J. P. Eboli, M. C. Gonzalez-Garcia and S. F. Novaes, Nucl. Phys. B **411**, 381 (1994) [hep-ph/9306306].
- [18] O. J. P. Eboli, M. B. Magro, P. G. Mercadante and S. F. Novaes, Phys. Rev. D **52**, 15 (1995) [hep-ph/9503432].
- [19] S. Dawson, A. Likhoded, G. Valencia and O. Yushchenko, eConf C **960625**, NEW147 (1996) [hep-ph/9610299].
- [20] G. Belanger, F. Boudjema, Y. Kurihara, D. Perret-Gallix and A. Semenov, Eur. Phys. J. C **13**, 283 (2000) [hep-ph/9908254].
- [21] G. Abbiendi *et al.* [OPAL Collaboration], Phys. Lett. B **471**, 293 (1999) [hep-ex/9910069].
- [22] M. Acciarri *et al.* [L3 Collaboration], Phys. Lett. B **478**, 39 (2000) [hep-ex/0002037].
- [23] J. Abdallah *et al.* [DELPHI Collaboration], Eur. Phys. J. C **31**, 139 (2003) [hep-ex/0311004].
- [24] G. Abbiendi *et al.* [OPAL Collaboration], Phys. Rev. D **70**, 032005 (2004) [hep-ex/0402021].
- [25] O. J. P. Eboli, M. C. Gonzalez-Garcia, S. M. Lietti and S. F. Novaes, Phys. Rev. D **63**, 075008 (2001) [hep-ph/0009262].
- [26] C. Royon, E. Chapon and O. Kepka, PoS DIS **2010**, 089 (2010) [AIP Conf. Proc. **1350**, 140 (2011)] [arXiv:1008.0258 [hep-ph]].
- [27] T. Pierzchala and K. Piotrkowski, Nucl. Phys. Proc. Suppl. **179-180**, 257 (2008) [arXiv:0807.1121 [hep-ph]].
- [28] A. Brunstein, O. J. P. Eboli and M. C. Gonzalez-Garcia, Phys. Lett. B **375**, 233 (1996) [hep-ph/9602264].
- [29] S. Godfrey, In *Los Angeles 1995, Vector boson self-interactions* 209-223 [hep-ph/9505252].
- [30] S. Chatrchyan *et al.* [CMS Collaboration], Phys. Rev. D **90** (2014) 3, 032008 [arXiv:1404.4619 [hep-ex]].
- [31] CMS collaboration, JHEP 07(2013)116 [arXiv:1305.5596]
- [32] ATLAS collaboration, ATLAS-CONF-2014-013
- [33] D. Yang, Y. Mao, Q. Li, S. Liu, Z. Xu and K. Ye, JHEP **1304**, 108 (2013) [arXiv:1211.1641[hep-ph]]

- [34] K. Ye, D. Yang and Q. Li, Phys. Rev. D **88**, 015023[arXiv:1305.5979[hep-ph]]
- [35] O. J. P. Eboli, M. C. Gonzalez-Garcia and J. K. Mizukoshi, [hep-ph/0606118].
- [36] C. Degrande *et al.* [arXiv:1309.7452[physics.comp-ph]]
- [37] O. Schlimbert and B. Feigl, "VBFNLO Utility to Calculate Form Factors", Karlsruher Institut fur Technologie,
<http://www.itp.kit.edu/~vbfnlweb/wiki/doku.php?id=download:formfactor>.
- [38] J. Wudka, eConf C **960625**, NEW176 (1996) [hep-ph/9606478].
- [39] Juan Alcaraz Maestre, Experimental limits on anomalous TGC couplings and future plans, Implications of LHC results for TeV-scale physics, CERN, Aug. 29 -Sep. 2, 2011.
- [40] J. Alwall, M. Herquet, F. Maltoni, O. Mattelaer and T. Stelzer, JHEP **1106** (2011) 128 [arXiv:1106.0522 [hep-ph]].
- [41] F. Maltoni and T. Stelzer, JHEP **0302**, 027 (2003) [hep-ph/0208156].
- [42] N. D. Christensen and C. Duhr, Comput. Phys. Commun. **180**, 1614 (2009) [arXiv:0806.4194 [hep-ph]].
- [43] C. Degrande, C. Duhr, B. Fuks, D. Grellscheid, O. Mattelaer and T. Reiter, [arXiv:1108.2040 [hep-ph]].
- [44] P. de Aquino, W. Link, F. Maltoni, O. Mattelaer and T. Stelzer, [arXiv:1108.2041 [hep-ph]].
- [45] T. Sjostrand, L. Lonnblad, S. Mrenna and P. Z. Skands, [hep-ph/0308153].
- [46] J. de Favereau *et al.* [DELPHES 3 Collaboration], JHEP **1402**, 057 (2014) [arXiv:1307.6346 [hep-ex]].
- [47] J. Anderson, *et al.* [arXiv:1309.1057[hep-ex]].
- [48] <http://madgraph.hep.uiuc.edu/Downloads/ExRootAnalysis>
- [49] R. Brun and F. Rademakers, Nucl. Instrum. Meth. A **389** (1997) 81.
- [50] B. Roe, H. Yang, J. Zhu, Y. Liu, I. Stancu, G. McGregor Nucl.Instrum.Meth. A **543** (2005) 577-584 [arXiv:physics/0408124]
- [51] A. Hoecker, P. Speckmayer, J. Stelzer, J. Therhaag, E. von Toerne, and H. Voss, PoS A CAT 040 (2007) [arXiv:physics/0703039].
- [52] Jadach, Stanislaw et al. Comput. Phys. Commun. **64**, 275 (1990). CERN-TH-5856-90.
- [53] J. Pumplin, D. R. Stump, J. Huston, H. L. Lai, P. M. Nadolsky and W. K. Tung, JHEP **0207**, 012 (2002) [hep-ph/0201195].